AIP | Journal of Applied Physics

Effect of capping material on interfacial ferromagnetism in FeRh thin films

C. Baldasseroni, G. K. Pálsson, C. Bordel, S. Valencia, A. A. Unal, F. Kronast, S. Nemsak, C. S. Fadley, J. A. Borchers, B. B. Maranville, and F. Hellman

Citation: Journal of Applied Physics **115**, 043919 (2014); doi: 10.1063/1.4862961
View online: http://dx.doi.org/10.1063/1.4862961
View Table of Contents: http://scitation.aip.org/content/aip/journal/jap/115/4?ver=pdfcov
Published by the AIP Publishing

Effect of capping material on interfacial ferromagnetism in FeRh thin films

C. Baldasseroni,[1,a)] G. K. Pálsson,[2,3] C. Bordel,[3,4,5] S. Valencia,[6] A. A. Unal,[6] F. Kronast,[6] S. Nemsak,[2,3] C. S. Fadley,[2,3] J. A. Borchers,[7] B. B. Maranville,[7] and F. Hellman[3,4]
[1]*Department of Materials Science and Engineering, University of California Berkeley, Berkeley, California 94720, USA*
[2]*Department of Physics, University of California, Davis, California 95616, USA*
[3]*Materials Sciences Division, Lawrence Berkeley National Laboratory, Berkeley, California 94720, USA*
[4]*Department of Physics, University of California, Berkeley, Berkeley, California 94720, USA*
[5]*GPM, UMR CNRS 6634, Université de Rouen, Av. de l'Université—BP12, 76801 St Etienne du Rouvray, France*
[6]*Helmholtz Zentrum-Berlin für Materialien und Energie GmbH, Albert-Einstein-Straße 15, D-12489 Berlin, Germany*
[7]*NIST Center for Neutron Research, National Institute of Standard and Technology, Gaithersburg, MD 20899, USA*

(Received 23 September 2013; accepted 9 January 2014; published online 31 January 2014)

The role of the capping material in stabilizing a thin ferromagnetic layer at the interface between a FeRh film and cap in the nominally antiferromagnetic phase at room temperature was studied by x-ray magnetic circular dichroism in photoemission electron microscopy and polarized neutron reflectivity. These techniques were used to determine the presence or absence of interfacial ferromagnetism (FM) in films capped with different oxides and metals. Chemically stable oxide caps do not generate any interfacial FM while the effect of metallic caps depends on the element, showing that interfacial FM is due to metallic interdiffusion and the formation of a ternary alloy with a modified antiferromagnetic to ferromagnetic transition temperature. © *2014 AIP Publishing LLC*.
[http://dx.doi.org/10.1063/1.4862961]

INTRODUCTION

Equiatomic FeRh was discovered in 1939 by Fallot *et al*. to undergo an unusual magnetic phase transition[1] later identified as a first order antiferromagnetic (AF) to ferromagnetic (FM) transition.[2,3] The existence of this transition just above room temperature (RT)—near 350 K—makes FeRh a unique model system, which is still of significant interest in the physics and materials science community.[4–9] It has been proposed as a candidate material for heat-assisted magnetic recording (HAMR), where it would be coupled to ferromagnetic layers,[10–12] as well as for magnetocaloric cooling. In most of the thin-film studies, both fundamental and applied, FeRh is capped with a thin film layer to protect against oxidation, commonly a noble metal (Au, Pt) or a light self-passivating metal such as Al. This is especially important for magnetic and structural studies based on surface-sensitive probes. However, a series of recent studies have shown that substrate and capping materials can induce interfacial effects where the magnetic properties of the FeRh film are modified near the interface with the capping layer as well as the substrate.[13–16] Specifically, a thin FM layer can be stabilized at temperatures where the stable phase in the bulk is AF, which we will refer to in this work as interfacial FM. These interfacial effects are directly relevant to the successful integration of FeRh in HAMR technology.

Interfacial ferromagnetism at RT has been previously observed by total electron yield x-ray magnetic circular dichroism (XMCD) in FeRh thin films capped with MgO and Au by Ding *et al*.[13] and by magnetic depth profile modeling of polarized neutron reflectometry (PNR) results in FeRh capped with MgO by Fan *et al*.[14] Both studies confirmed the presence of interfacial FM near the top interface, but with a highly reduced magnetic signal compared to that of a fully FM film at 400 K. The interfacial FM was attributed to a combination of the effect of strain and Fe deficiency causing a mixed state of FeRh CsCl (FM) and Rh-rich fcc (PM) phases with reduced moment and a lowered AF-FM transition temperature T_0 compared to the single FeRh CsCl phase. For the film capped with MgO, an extremely weak interfacial moment of 0.02 μ_B/atom (compared to 1.56 μ_B/atom for FM film at 400 K) is estimated.

Our group recently reported on interfacial FM observed at RT with XMCD-photoemission electron microscopy (PEEM) on FeRh films capped with Al; these films are nominally AF at RT according to magnetometry characterization.[15] The interface with the FeRh native oxide of an uncapped film was by contrast found in our previous work to be non-magnetic.

Finally, Loving *et al*.[16] used diffusion from an Au capping layer to tune T_0 of FeRh thin films, showing that a structure with a magnetization gradient as a function of depth can be created. In particular, they found interfacial FM in films where the FeRh and Au had been deposited at high temperature, thereby allowing interdiffusion between the two.

These previous works point to effects coming from a combination of strain, Fe deficiency, and chemical diffusion from the cap but the variety of systems studied and experimental techniques used renders the interpretation difficult. A

[a)]Author to whom correspondence should be addressed. Electronic mail: cbaldasseroni@berkeley.edu

systematic study of the effect of different materials is required to elucidate the role of chemical diffusion and is the focus of this paper.

As background, T_0 has been shown to be sensitive to small changes in at. % Rh composition as indicated in the reported phase diagrams for the Fe-Rh system[17,18] constructed from data on bulk samples. The effect of the composition on T_0 (here defined as the average of $T_{AF\text{-}FM}$ and $T_{FM\text{-}AF}$) has been reported in thin films as well.[19,20] In particular, we have observed a significant reduction of 10 K per 1 at. % Rh composition change (C. Baldasseroni, C. Bordel, F. Hellman 2013) (from 397 K at 48.5 at. % Rh to 367 K at 51.5 at. % Rh). For lower Rh concentration, we found that alloys with composition $\leq$47.5 at. % Rh are FM from 300 K to 10 K, in good agreement with the existing phase diagrams indicating that the AF phase exists only over a small composition range near equiatomic. Deviations from equiatomic composition of a few at. % can thus significantly lower T_0 or even stabilize the FM phase over the entire temperature range.

Doping with small amounts (1 to 10 at. %) of ternary metallic elements also affects this sensitive system.[21–25] Some elements such as Ni, Pd and Al, lower T_0, while others such as Ir and Pt raise it. An overview of the effects due to doping with different metals can be found in the recent work of Barua *et al.*[26]

An increased T_0 (near 500 K for 5 to 10 at. % Pt) improves the suitability of FeRh for magnetic recording.[11,27] In addition, the likely high anisotropy FM media that FeRh would be coupled to is FePt, and therefore understanding the effect of Pt diffusion on interfacial FeRh is crucial.[24,27,28] This doping effect is expected if Pt or another metallic capping element diffuses into the FeRh film, thereby modifying the transition temperature T_0 of the interfacial layer.

In this work, we use a surface sensitive magnetic spectromicroscopy technique to directly probe the magnetic structure in the region near the interface with different capping layers and polarized neutron reflectivity to characterize the magnetic profile of the different samples as a function of depth to understand the origin of the interfacial effects. In an effort to focus on the chemical effects such as species segregation and diffusion at the interface, we systematically studied 5 different capping materials. Due to the differences in cap material, growth modes, and small variations in cap thicknesses, a constant strain state is not guaranteed between the different samples. Nevertheless, attempts were made at minimizing differences in strain state by keeping the thickness of the cap small (1.8 to 2.5 nm) compared to the thickness of the FeRh layer of $\sim$100 nm and depositing all caps at RT to eliminate differential thermal expansion between the two layers. All films were grown at the same temperature and on the same type of substrate.

The 5 different caps studied were: Al, Pt and Ag, FeRh native oxide, and alumina. The effect of alumina caps with two different thicknesses (1.8 and 2.5 nm) was also studied to look for a strain effect. XMCD-PEEM was used systematically on all 5 different caps to probe the magnetism at the interface between the FeRh and the cap. PNR was used as a complementary technique to get depth resolution for two of the films capped with metallic layers (Al and Ag).

EXPERIMENTAL METHODS

Thin films of FeRh (001) with $\sim$100 nm thickness were grown by magnetron sputtering from a FeRh alloy target onto (001) MgO substrates. The base pressure in the chamber was 8×10^{-8} Torr. The growth was performed at a substrate temperature of 873 K, using a DC power of 40 W, and an argon pressure of 2 mTorr. The growth rate measured by a quartz crystal microbalance was 0.04 nm/s. The films were subsequently given one of the following treatments: (1) left uncapped to allow the formation of a native oxide with a thickness estimated by hard x-ray photoemission spectroscopy measurements to be less than 2 nm, (2) capped *in-situ* (without breaking high vacuum) with 1.8 nm or 2.5 nm of alumina by reactive sputtering from an Al target, or with 1.8 nm of sputtered Pt, (3) capped *ex-situ* (after exposure to atmosphere) with 2.5 nm of sputtered Al or with 2.5 nm of sputtered Ag. Note that all capping depositions were done at RT to minimize interdiffusion between the FeRh film and the capping layer and to eliminate differences in strain induced by differential thermal contraction of cap and FeRh. The films capped without breaking high vacuum were allowed to cool to RT (2 h minimum) before subsequent deposition, therefore resulting in a similar potential exposure to water and other oxidants as the films capped after exposure to atmosphere (a monolayer of adsorbed gas molecules is formed on the surface of the FeRh film in less than 30 s at 8×10^{-8} Torr). Hence, in this work, we do not distinguish between capped *ex-situ* and *in-situ*. The thickness of the deposited caps was controlled based on the calibrated rate of deposition of each material (thickness of calibration films measured by profilometry).

The magnetic phase transition of all samples was measured by SQUID magnetometry. Figure 1 shows the temperature dependence of the magnetization (normalized between 0 and 1) of the 5 different samples in an applied field of 5 T. By correcting for the effect of the applied magnetic field on the transition temperature (-8 K/T, determined experimentally on an uncapped FeRh film grown under the same conditions), we find that all 5 samples are fully AF below 340 K and fully FM above 410 K in zero applied magnetic field. The spread in transition temperature observed between the 5 different samples is attributed to the extreme sensitivity of T_0 on factors such as small changes in Fe composition. Indeed, a measured composition shift of 2 at. % between different samples is due to the drift in sputter target composition over time because of non-equal sputtering yields between Fe and Rh species. T_0 follows the expected trend of decreasing with increasing Rh concentration. Note that SQUID magnetometry measurements of $M(H)$ at 300 K show a small non-zero magnetization indicative of a residual FM component in all films. A saturation magnetization of 80 to 100 emu/cc is measured at 300 K, 7 to 10% of the fully FM state at 400 K (not shown). Since SQUID magnetometry is not a local technique, we cannot determine whether this contribution is distributed through the film, originates from either the top or bottom interface, or if it is a combination of both. A surface sensitive or depth sensitive technique is necessary to distinguish between these.

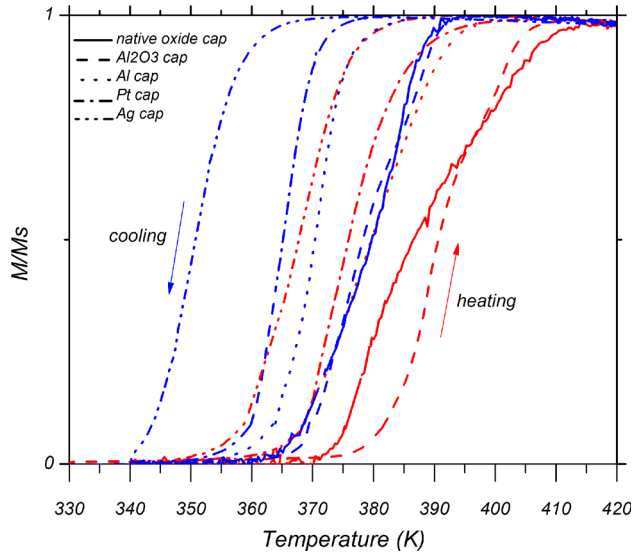

FIG. 1. Temperature-dependent magnetization of FeRh films with different caps showing the hysteretic transition from AF (near zero magnetization) to FM phase. The transition was measured in an external field of 5 T and the temperature axis has been corrected to reflect the transition in no external field since that is what is measured in both PEEM and PNR. Note that all films are fully FM above 410 K and fully AF below 340 K. M is normalized by its high T, fully FM value to account for small differences in composition. Different line types are used to distinguish the different samples and red/blue colors are used to distinguish the heating/cooling curves.

Table I summarizes the structural and chemical information of the different FeRh/cap systems. The structural and chemical ordering quality of each film was checked by x-ray diffractometry and showed small deviation in the mosaicity and coherence length between the different films with respective average values of $0.34 \pm 0.02^{\circ}$ and 35 ± 1 nm, as well as similar lattice parameters indicating a cubic structure with negligible tetragonal strain within our measurement accuracy ($\pm 0.3\%$). The chemical order parameter S, defined as the corrected ratio of 001 to 002 Bragg peaks integrated intensities $S = \sqrt{I_{001}/I_{002}}_{exp} / \sqrt{I_{001}/I_{002}}_{calc}$, determined on separate uncapped FeRh films grown under the same condition is $S = 0.88 \pm 0.03$ (average of 3 films in the composition range 49 to 51.4 at. % Rh). The calculated theoretical intensities include corrections for the structure factor, the polarization factor, the Lorentz factor, the absorption factor, and the temperature factor (see Refs. 29 and 30). The film and cap thicknesses and the roughness of the interface were determined by x-ray reflectivity. The Al and alumina caps are thicker than nominal thickness based on Al deposition rate due to the oxidation of the Al. The interface roughness of the films is similar for all samples (1–4 nm), in good agreement with the topography of uncapped FeRh films measured by atomic force microscopy which shows rms roughness of ~5 nm. Note that the reflectivity model does not distinguish between a topographically rough interface and a chemically diffuse interface, and therefore both could contribute to the measured roughness. An accurate value of the roughness of the interface and cap thickness could not be determined from the x-ray reflectivity model fit for the FeRh film capped with Pt (non-detectable oscillations possibly due to a non-uniform Pt film or Pt islands), so the cap thickness value reported in Table I is the nominal deposition thickness. The composition of the FeRh films was measured by Rutherford backscattering spectrometry.

XMCD in PEEM is a surface-sensitive magnetic microscopy technique suitable for the study of interfacial magnetic phenomena in buried layers due to its element selectivity and the penetration of the x-ray photons. The probing depth is the distance at which the recorded intensity decreases by a factor of e and is typically around 5 nm in metallic samples. The intensity from a buried layer signal decreases exponentially with thickness but can be measured by increasing the integration time. In the samples studied here, all sample-cap interface regions were within the probing depth.

XMCD-PEEM imaging was performed at HZB beamline UE49-PGM-a-SPEEM, which is equipped with an Elmitec PEEM III microscope, at the Fe L_3 edge (705.6 eV), using low-energy secondary electrons with a spatial resolution of ~30 nm. Magnetic contrast images were computed as described in Ref. 15 by plotting the XMCD asymmetry from left and right circularly polarized radiation at the Fe L_3 edge. XMCD asymmetry is proportional to the projection of the magnetization along the propagation direction of the incoming x-ray beam. Saturated blue (red) in the selected color scale highlights magnetic domains with a projection of the magnetization aligned parallel (antiparallel) to the propagation direction of the photons. The color gradient indicates a lower magnetization or a rotation of the local magnetization direction away from the x-ray beam direction. No external magnetic field was applied during the measurement. Images were recorded in the initial RT state (nominally AF), then in the fully FM phase between 400 K and 420 K and finally at RT again to check the stability of the initial interfacial phase.

PNR was performed on the MAGIK reflectometer at the NIST Center for Neutron Research as a function of temperature in order to fully characterize the depth-dependence of the magnetization.[31] Spin-polarized neutrons were specularly

TABLE I. Summary of films and caps structural and chemical parameters.

Sample No. and cap	Nominal cap thickness (nm)	Rh composition (%)	c (nm)	a (nm)	c/a (%)	Coherence length (nm)	Mosaicity (deg)	Film thickness (nm)	Cap thickness (nm)	Cap-film interface roughness (nm)
S11-090 no cap	N/A	50.4	0.2988	0.2990	99.9	34	0.33	95	N/A	N/A
S11-090 Al	2.5	50.4	0.2988	0.2990	99.9	34	0.33	95	5.6	1.5
S12-011 Pt	1.8	51.2	0.2982	0.2992	99.7	36	0.32	110	1.8	N/A
S12-054 alumina	2.5	51.5	0.2983	0.2990	99.8	34	0.38	97	7.5	3.8
S13-008 Ag	2.5	52.5	–	–	–	–	–	103	7.3	4.3

reflected from the sample in an applied field of 0.68 T at 450 K in the nominally FM phase and 300 K in the nominally AF phase. At each temperature, all four cross sections (non-spin flip and spin flip) were measured as a function of wave vector Q. Beam footprint and polarization efficiency corrections were applied to the raw data. No features were observed in the spin flip cross sections, confirming that all the magnetizations are in the plane of the film, parallel to the applied field. The resultant non-spin flip cross sections ($--$ and $++$) at both temperatures were fit to a model for the chemical and magnetic scattering length density (SLD) depth profiles for the stack MgO/FeRh/cap in order to isolate the magnetization near the bottom and top interfaces of the FeRh film at RT. Thickness and roughness values from the x-ray reflectivity data summarized in Table I were used as initial values for the PNR fit. The FeRh layer was divided into 3 layers with different magnetic SLDs and the model was then fit to the experimental data using the refl1D PNR software.[32] The data at different temperatures were fit simultaneously, with the chemical SLDs, layer thicknesses, and interface roughnesses kept constant between the two temperatures and only the magnetic SLDs allowed to vary.

RESULTS

Figure 2 shows images of the XMCD asymmetry corresponding to the interfacial FeRh phase at different temperatures for the FeRh thin film capped with Al. Similar to other studies with a Au capping layer,[13,16] we find that the Al cap induces a RT FM interfacial layer that is stable to thermal cycling. The interfacial FM at RT (Fig. 2(a)) has a reduced contrast compared to the fully FM phase above T_0 (Fig. 2(b)), but is clearly visible.

Changes in XMCD-PEEM magnetic contrast can generally be attributed to 3 separate factors: the magnitude of the Fe moments, the fraction of Fe atoms within the probing depth that carry a FM moment, and the direction of the Fe moments. It is unlikely that the direction of the Fe moments plays a role in reducing the signal, since these films are unstrained and there is no reason for the moment of the FM layer to point substantially out of the plane. Metallic doping by a non-magnetic element has been shown to reduce the Fe magnetic moment in FeRh[16,21–23] and is the most likely factor. The observed reduced magnetic signal of the RT interfacial FM compared to the fully FM phase can also be the result of a thin FM layer compared to the probing depth of ca. 5 nm, or a combination of these two factors. We used PNR to separate these two factors and determine the thickness of the interfacial FM layer giving rise to this signal and the magnitude of the magnetic moment carried in this layer.

Figures 3(a) and 3(b) show the resultant non-spin flip cross sections ($--$ and $++$) at both temperatures and Figs. 3(c) and 3(d) show the corresponding structural and magnetic layer models of the stack MgO/FeRh/Al fit to the reflectivity data.

Our structural and magnetic layers model is in excellent agreement with the high temperature PNR experimental data. The magnetic moment per FeRh atom of the fully FM layer in this model is 1.61 μ_B, in good agreement with the saturation magnetization of 1.77 μ_B measured by magnetometry. The model is also in good agreement with the RT data. It requires the presence of a non-negligible magnetic layer at the interface between the FeRh layer and the Al cap at room temperature. The interfacial magnetic layer is modeled to have a thickness of 7 nm with a magnetic SLD of 0.50×10^{-6} Å^{-2}, which corresponds to a magnetic moment of 0.23 μ_B; this reduced moment deduced from PNR is consistent with the reduced asymmetry of the RT XMCD-PEEM image (± 0.05) of this sample compared to the asymmetry at 400 K (± 0.15).

In addition, the PNR reveals that there is a magnetic layer at the MgO/FeRh substrate interface as shown by the magnetic SLD in Fig. 3(d) and in good agreement with previous observations in Ref. 14. This magnetic layer can be attributed to a Rh-rich layer near the bottom interface as suggested in Ref. 16. Indeed, both the x-ray reflectivity and PNR fits are improved by inclusion of this Rh-rich bottom layer. For the PNR fits, this is shown in the small dip in the structural profiles near the substrate and the cap in Figs. 3(c) and 3(d). Near the substrate, we speculate that this variation in the FeRh composition with depth is due to Fe deficiency because of Fe diffusion into the MgO substrate. Interfacial diffusion between Fe and MgO has been reported in studies related to magnetic tunnel junctions with formation of an inter-diffused (Mg,Fe)O layer at the interface after annealing to temperatures above 450 °C.[33,34] Our films are deposited at 600 °C and a similar effect would result in Fe depletion in the bottom layer, therefore increasing the Rh concentration locally. As discussed in the introduction, an increase in Rh concentration lowers T_0 and can lead to the stabilization of the FM phase at RT. At the upper interface, near the cap, either Rh enrichment in FeRh due to Fe diffusion into the Al

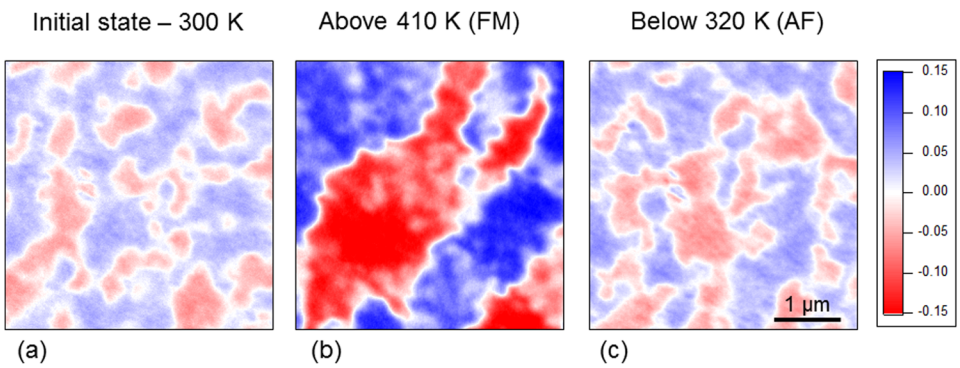

FIG. 2. XMCD-PEEM asymmetry images of FeRh thin film capped with Al at (a) the initial room temperature state, (b) above 410 K in the fully FM phase, (c) cooled back below 320 K in the nominally AF phase. The interfacial FM layer is stable to temperature cycling. The labels (FM) and (AF) indicate the nominal phase according to bulk magnetization measurements.

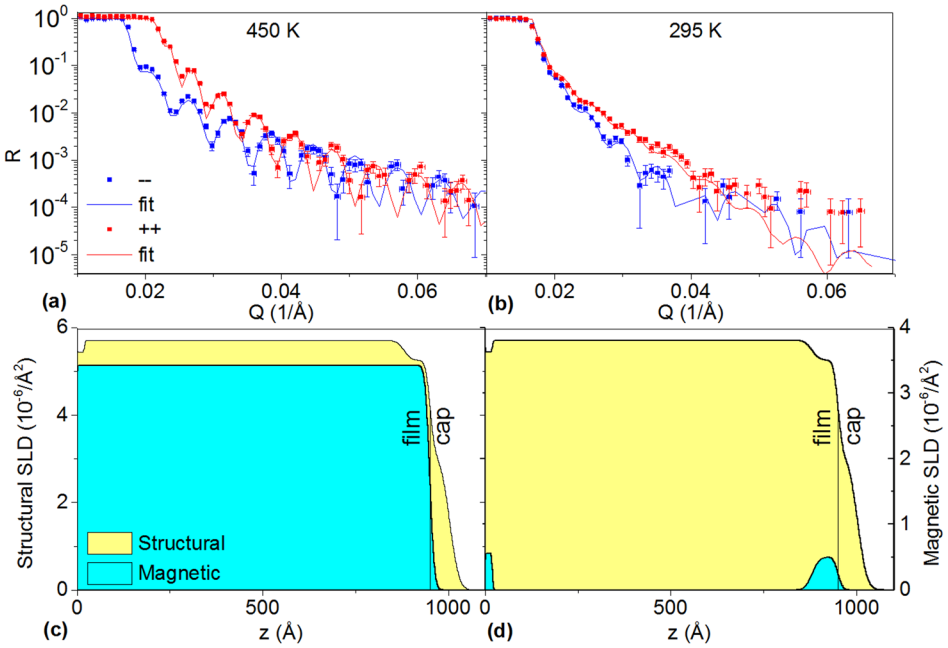

FIG. 3. PNR reflectivity curves for FeRh capped with Al at (a) 450 K (fully FM) and (b) 295 K (interfacial FM only) and corresponding structural and magnetic profile models (c) and (d).

cap or Al diffusion into and consequent doping of FeRh can account for the reduction in SLD and the stabilization of a FM layer.

Note that the magnetic moment of 0.23 μ_B, found at the interface with the Al cap, is an order of magnitude larger than the interfacial FM reported by Fan *et al*. of 0.02 μ_B for a FeRh film capped with the oxide MgO,[14] indicating that the effect of Al on the interfacial FM is stronger than that of an MgO cap.

In order to further compare the effect of an oxide to that of Al, a FeRh film capped with alumina was studied. Figure 4 shows the magnetic contrast images of the FeRh film capped with alumina. A surprising behavior is observed: interfacial FM is seen initially at RT and disappears after the first heating-cooling cycle and subsequent temperature cycles. The FeRh film capped with a thinner alumina layer (nominal 1.8 nm compared to 2.5 nm) shows the same behavior. X-ray photoemission spectroscopy (XPS) of the sample performed in the PEEM microscope chamber reveals that the alumina cap is initially not chemically homogeneous: it contains oxidized and metallic aluminum atoms. The initial FM interface is attributed to the presence of some metallic Al at the interface, which upon small heating reacts with and is incorporated into the alumina cap.

To confirm our explanation of the alumina cap, we turn to x-ray photoemission spectroscopy (XPS), specifically a detailed analysis of the XPS Al, Fe, and Rh peaks, before and after heating this alumina capped sample. A systematic XPS study is beyond the scope of the present work. Figure 5(a) shows the Al 2p XPS peaks measured before and after heating. A strong presence of metallic Al is seen before heating as indicated by the double peak structure that has been fit with two components. A rough estimate gives that only 50% of the layer is initially oxidized. After heating, only one chemical state is observed in Al 2p XPS peak within our resolution limit, associated with alumina. Each spectrum was calibrated using the C 1s peak but a small residual energy shift is seen between the two spectra, due to a different band alignment as confirmed by the binding energy of the O 1s peak (not shown). The small feature seen in both spectra at higher binding energy corresponds to the Rh 4s XPS peak. Further comparison of the XPS spectra before and after heating shows that the Fe and Rh elemental peaks have a reduced amplitude after heating (Figures 5(b) and 5(c)), indicating that the thickness of the capping layer is increasing, in good agreement with the formation of more oxide (~1 nm of extra alumina cap as estimated from the magnitude of the reduction). Note that a change in

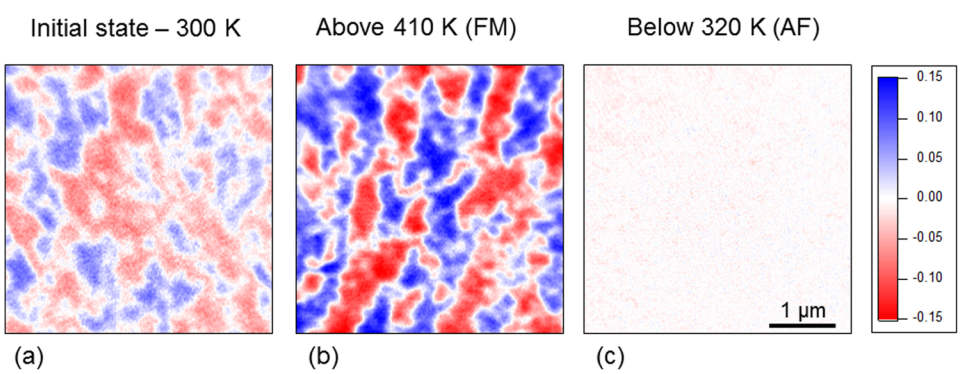

FIG. 4. XMCD-PEEM asymmetry images of FeRh thin film capped with alumina at (a) the initial room temperature state, (b) above 410 K in the fully FM phase, (c) cooled back below 320 K in the fully AF phase. While initial FM domains are seen in the room temperature image (a), after heating to the fully FM phase and cooling back below the transition temperature no interfacial FM persists and instead a fully AF interface is seen. This AF phase is stable to further heating and cooling cycles.

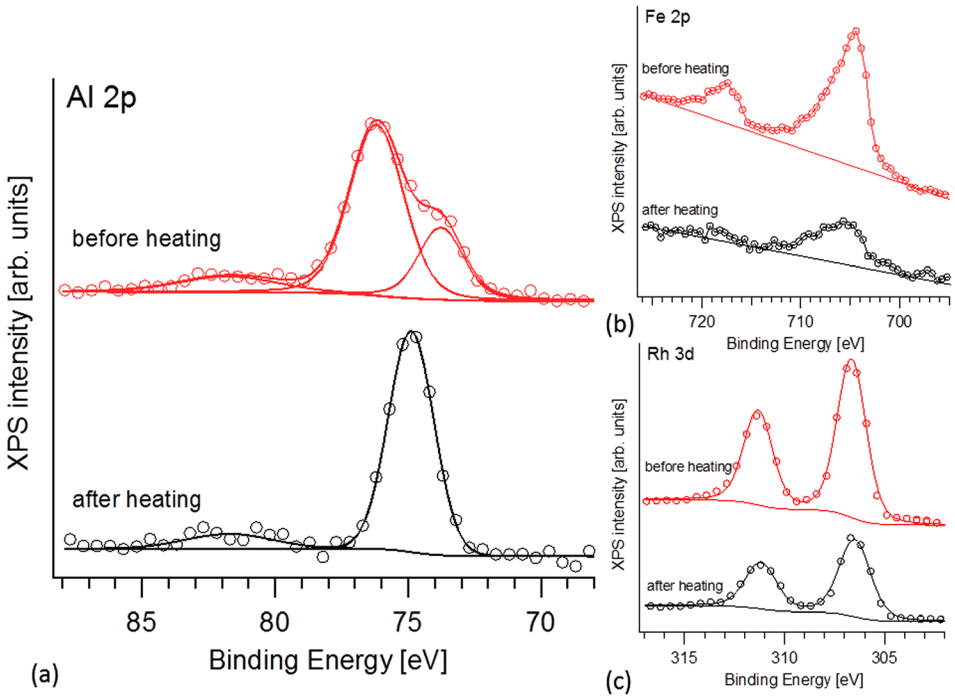

FIG. 5. XPS spectra of FeRh thin film capped with alumina recorded at room temperature in the initial state (before heating) and after a full cycle of heating above 410 K and cooling back to room temperature (after heating), showing the details of (a) the Al 2p peak, (b) the Fe 2p peak, and (c) the Rh 3d peak.

morphology of the cap could cause additional damping of the Fe and Rh peaks.

To support our claim that a stable, fully oxidized cap does not generate any interfacial FM, we turn to an uncapped film that was previously studied for the nucleation and growth of the FM phase.[15] This film is effectively capped with a native oxide. Hard x-ray photoemission spectroscopy of the Fe 2p and Rh 3d core levels (data not shown here) reveals that Rh is present in the metallic state only and that the native oxide is composed of Fe oxide. The most probable candidate according to the structure of the Fe 2p peak is Fe_2O_3, with an estimated thickness of 2 nm.

Figure 6 shows the magnetic contrast images recorded during the full heating and cooling cycle (AF, FM, AF again) of the film capped with native oxide. No detectable FM phase is observed at the interface with the native oxide. A structure of large FM domains with strong contrast is observed in the fully FM phase at 415 K, similar to the structures seen in the film capped with Al and alumina. After cooling, a weak residual magnetic contrast is detected locally where the FM islands last disappeared but the majority of the background has no asymmetry, indicating its AF nature. The weak residual magnetic contrast is in agreement with the FeRh/MgO cap interfacial FM signal of 0.02 μ_B reported by Fan *et al.*[14]

To further investigate the effect of a metallic cap, Figure 7 shows the asymmetry images of a FeRh film capped with Pt. Unlike the film capped with the other metallic layer of Al, no interfacial FM is observed at RT, both in the initial state and after a full heating and cooling cycle. In the fully FM phase, the typical pattern of FM domains with strong FM contrast is seen again (the quality of these images is slightly reduced due to a lower acquisition time). Even in the case of a non-uniform film due to the formation of Pt islands, this shows that in the regions covered with Pt, the Pt results in the same absence of interfacial FM as the native oxide cap.

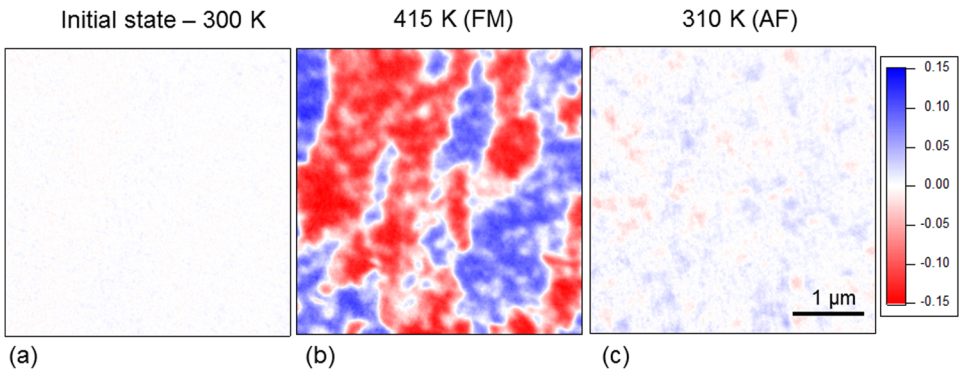

FIG. 6. XMCD-PEEM asymmetry images of uncapped FeRh thin film, effectively capped with a native oxide of 2 nm or less at (a) the initial room temperature state, (b) 415 K in the fully FM phase, (c) cooled back to 310 K in the fully AF phase. The white color in the low temperature images (a) indicates the absence of FM domains, while the 415 K image (b) shows a strong FM contrast. A weak residual magnetic contrast is detected in some areas in (c) but the majority of the background is white, indicating the AF phase is recovered after cooling to 310 K.

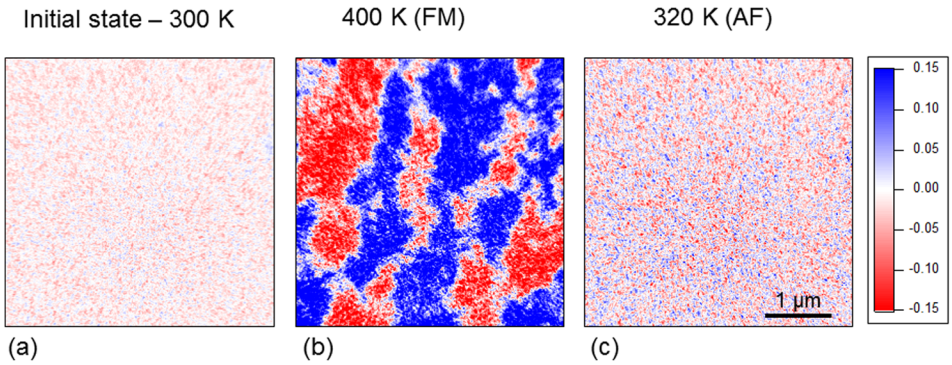

FIG. 7. XMCD-PEEM asymmetry images of FeRh thin film capped with 1.8 nm of Pt at (a) the initial room temperature state, (b) 400 K in the fully FM phase, (c) cooled back to 320 K in the fully AF phase. Note that the initial and final images show only noise, so there is no interfacial FM at room temperature. Lower acquisition time is responsible for the increased pixelation noise seen in all three images.

Finally, PNR measurement of a FeRh film capped with Ag was performed. The same methodology as for the Al-capped film was used to perform the measurement and analyze the data. Figure 8(a) shows the non-spin flip cross sections at RT. The reflectivity data recorded at 450 K (not shown) is very similar to the film capped with Al and modeled with a fully FM layer of magnetic moment 1.60 μ_B (lower than that for the film capped with Al due to a lower Fe concentration within the film overall). When comparing the RT reflectivity profile of the film with Ag cap to the Al capped film, it is clear that while the Al capped films showed a strong splitting between the $++$ and $--$ cross sections indicating the presence of FM at RT, splitting in the Ag capped film is minimal (close to the resolution limit), indicating that the magnetic signal at RT is negligible. Indeed, a reasonable fit is obtained by assuming a model with no interfacial FM layer at the interface with the Ag cap at RT, as shown in Fig. 8(b). In the structural profile, although a slightly reduced SLD layer near the top interface improves the model, as in the case of the Al capped sample, here no sharp dip in SLD is apparent at the top interface, and the top layer shows a significantly longer "tail" of SLD, consistent with a rough interface between FeRh and Ag and a rough Ag surface layer.

At the bottom surface, the data for the two films are very similar, showing a FM component at RT and a dip in the structural density. Our data thus indicate that the magnetic component that gives rise to the small splitting between $++$ and $--$ is located at the bottom interface with the MgO substrate, consistent with the observation for the Al-capped film. In both samples, the bottom FM layer is ~2 nm thick with a moment of 0.26 μ_B.

XMCD-PEEM of the FeRh/Ag interface near RT is in good agreement with the PNR results as shown in Fig. 8(c), confirming the absence of interfacial FM. Note that the combination of the large roughness of the cap from the x-ray reflectivity and PNR models and the detection of some oxidation in XPS of this film capped with Ag indicates the possibility of a non-uniform island forming cap, similar to the Pt cap. But since PNR information is averaged over the entire sample surface area and the field of view of the XMCD-PEEM image is 4 μm, assumed to be large compared to the typical size of islands, the FeRh/Ag interface was clearly probed in our measurements and was not magnetic.

DISCUSSION

The data indicate a FM signal at RT for all samples at the FeRh/MgO (substrate) interface, accompanied by a dip

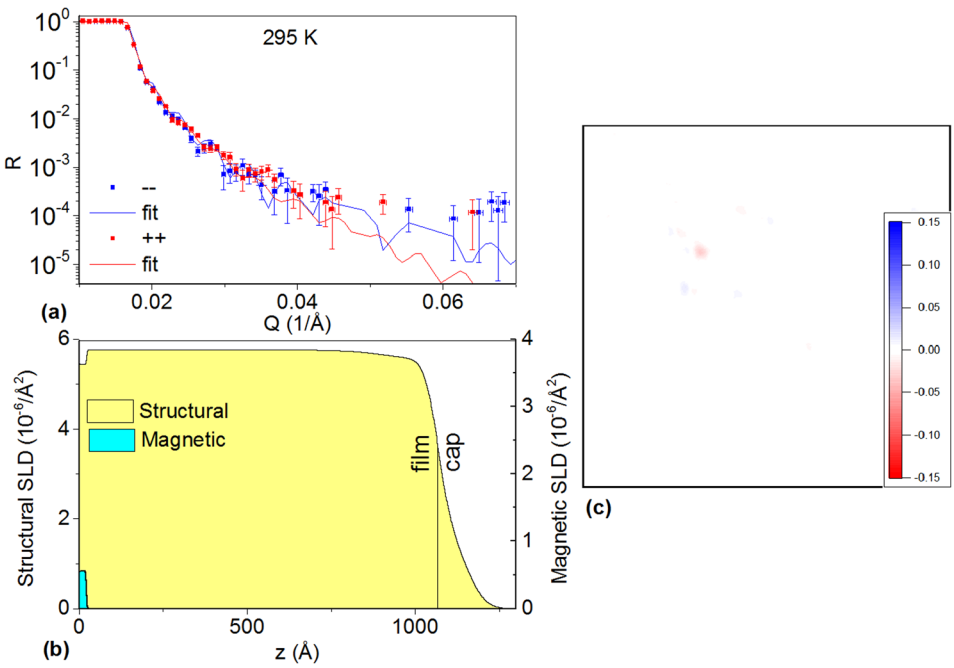

FIG. 8. (a) Room temperature PNR reflectivity curves for FeRh capped with Ag and (b) corresponding structural and magnetic profile models. (c) XMCD-PEEM asymmetry image of FeRh capped with Ag near room temperature showing the mostly AF interface (except for a few weak residual local FM domains).

in SLD, which is consistent with diffusion of Fe into the MgO substrate, leaving behind a Rh-rich layer. At the top interface, with the capping layer, a variety of results are seen. We suggest all data can be explained by considering diffusion of metallic caps into FeRh, which modify T_0. The Al cap (known to reduce T_0 (Ref. 25)) produces a FM interfacial layer, Pt (known to raise T_0 (Refs. 21–24)) and Ag (non-miscible[22]) both yield non-magnetic interfaces at RT, but for different reasons.

Diffusion of Al from the Al cap into the FeRh film during the growth results in a lightly Al-doped FeRh layer near the interface with the cap, thereby lowering T_0 of this interfacial layer and making the FM phase stable at RT at the interface, as observed by XMCD-PEEM and PNR. For the Pt cap, the miscibility of Pt in FeRh (and of Fe in Pt) suggests that interdiffusion occurs, as it does with the Al cap, but because the effect of Pt in FeRh is to increase T_0, unlike Al which decreases it, interdiffusion would leave the interface layer AF at RT as is seen experimentally. The increase of T_0 induced by Pt doping is well-documented and ranges from 7 K to 20 K per at. % of Pt.[21–24] Since the XMCD-PEEM signal at 400 K for the Pt capped films is of the same intensity as the other films, $T_{AF\text{-}FM}$ of the interface layer could have been increased by Pt interdiffusion but must be less than 400 K. Alternatively, it is possible that Pt does not interdiffuse at RT. For technological use of FeRh in which maintaining the magnetic properties of FeRh at the interface is desired, the selection of an immiscible element such as Ag or Re[22] as the cap material would prevent interfacial FM in FeRh. Ag is not miscible and therefore has no effect on the magnetic properties of FeRh, as shown. Both oxide caps (fully oxidized alumina and native oxide) do not induce any RT interfacial FM due to the absence of metallic element diffusion. As shown by the XPS analysis, the initial FM seen at the interface with the non-fully oxidized alumina cap is due to some residual metallic Al in the cap; this FM layer goes away on cycling due to complete oxidation of the Al cap.

Another possible source of interfacial FM could be the stabilization of a layer with different FeRh composition from the bulk, either due to a single-species termination of the surface/interface or because of surface/interface segregation. The films studied in this work have [001] direction out of the plane, therefore we are interested in the properties of {001} surfaces. In a perfect equiatomic alloy, this surface consists of alternating Fe and Rh layers and is terminated by a layer of only one species. Rh termination of the {001} surfaces in FeRh was experimentally observed by quantitative low energy electron diffraction (LEED) by Kim *et al.*[35] Based on this observation, Lounis *et al.*[36] performed theoretical density functional theory calculations and showed that, for films below a certain thickness, the 100% Rh-terminated (001) surface results in a magnetic reconstruction which stabilizes the FM phase near the surface. Their calculation shows that the 100% Fe-terminated surface does not cause any magnetic surface reconstruction. However, the stability of the Rh termination versus the Fe termination was not studied. Several groups have relied on this theory to explain the experimental observation of a residual FM component at RT,[37–39] including the interfacial studies already mentioned.[13,14]

While there is some experimental evidence for preferential Rh termination of the FeRh (001) surface, no direct experimental reports of surface segregation leading to a local increase of Fe or Rh concentration could be found. Theoretical calculations of surface segregation energies in transition-metal alloys by Ruban *et al.*[40] predict a strong surface segregation of Rh in Fe for a bcc (001) surface but this calculation assumes that Rh is a dilute impurity and care must be taken when comparing this result to a concentrated equiatomic alloy of Fe and Rh as segregation reversal is seen in other concentrated systems. Indeed, Heinz and Hammer[41] report experimental results on the ordered B2 FeAl alloy and show that the segregation question is quite rich and complicated. In summary, three general cases are possible: (1) the ordered bulk-like termination is favored, (2) chemical disorder is induced in the first few surface layers, or (3) a new kind of chemical order can develop. This latter case is often the result of surface preparation (sputtering and annealing) inducing a metastable state. In particular, the Rh termination observed by LEED in Ref. 35 could be the result of the cleaning procedure that the sample experienced. In contrast, a recent surface-sensitive photoemission study of ultrathin FeRh films deposited *in-situ* by Lee *et al.* reported no significant change in Rh to Fe core level photoemission intensity ratio after annealing the film, indicating no strong tendency of surface segregation of either Fe or Rh.[42]

Heat treatment of the film can also modify the surface. We have observed in XMCD-PEEM of uncapped films with an initial AF surface that after heating above the Curie temperature of 573 K the surface of the film is modified and remains FM at RT on cooling. The same effect was observed on a film with higher Rh concentration heated only to 395 K for several hours. These films have not been examined in detail, but based on the observations in this paper the FM layer near the surface is likely due to Rh-enrichment caused by diffusion, possibly associated with surface segregation or increased oxidation of the surface, although the annealing was done in high vacuum.

Finally, the adsorption of atoms of a third species can modify the segregation or reconstruction expected in equilibrium with the vacuum. This means that capping with different materials could lead to different segregation configurations. A possible illustration was recently reported by McLaren *et al.*[43] The composition profile along the cross-section of a 50 nm FeRh film capped with Al shows the presence of a Fe-rich region extending to about 2 nm below the FeRh/Al interface. This result indicates that the Al cap favors Fe segregation at the interface, contrasting with the Rh termination of an Ar-ion-bombarded surface and the absence of segregation of the surface of an *in-situ* deposited film.

Since both Fe segregation and Rh termination could result in the stabilization of a FM layer at the interface, one would expect a FM interface to always be observed. However, our results show that this is not the case. In particular, the uncapped film was found to have a native oxide layer at the surface, consisting of Fe oxide. The formation of Fe oxide causes some Rh-enrichment of the top FeRh layer near the interface with the native oxide, but no interfacial

FM was found, indicating that this Rh-enrichment is not sufficient to generate interfacial FM. Therefore, we suggest that segregation effects are secondary and that the main driving force for the stabilization of FM is the alloying with the third metallic element from the cap.

Comparison of alumina caps of different thickness eliminates strain as the main cause. A FeRh film capped with a thinner alumina layer (nominal 1.8 nm compared to 2.5 nm) shows the same behavior as seen in Fig. 4 (some initial interfacial FM that disappears after the first heating/cooling cycle). This confirms that strain resulting from capping layers of different thicknesses is not enough by itself to generate interfacial FM.

These results show that chemical effects alone can explain the stabilization of an interfacial FM layer at RT in FeRh capped with Al. The opposite effect of capping with a different soluble metallic element (Pt) is clear evidence of the chemical origin of the FM layer and confirms our hypothesis. In particular, in the case of the Al cap, Al diffusion into the FeRh layer is consistent with the reduced SLD near the top interface seen in the PNR model. Note that the PNR structural SLD model does not give any evidence for the Fe segregation observed in Ref. 43.

CONCLUSION

In conclusion, our results show that chemical interdiffusion accounts for interfacial FM in FeRh thin films at both the bottom and top interfaces. Interfacial FM seen at the bottom FeRh interface with the MgO substrate is likely due to Rh-enrichment. Interfacial FM at the top interface with caps depends on the capping material and was systematically studied for 5 different capping materials (native oxide, alumina, Al, Pt, and Ag). While no measurable interfacial FM is seen at the interface with stable oxide caps, XMCD-PEEM and PNR confirm that Al stabilizes a FM layer of ~7 nm with magnetization reduced by a factor of 7 with respect to the nominal FM film. No such layer is seen for Pt or Ag. The FM interface layer is the result of alloying between FeRh and the cap element. Al doping acts to lower T_0 while Pt raises it. Ag is not miscible therefore has no effect on the magnetic properties of FeRh. Understanding of the chemical interdiffusion origin of interfacial FM in FeRh enables improvements in the technological implementation of FeRh. In particular, the use of non-miscible layers is recommended to limit interdiffusion between the metallic layers and to maintain the nominal magnetic properties of the FeRh film or, when not possible, the change in magnetic properties of FeRh must be taken into account.

ACKNOWLEDGMENTS

We thank A. X. Gray, A. M. Kaiser, J. Herrero-Albillos, and C. M. Schneider for help with the PEEM measurements, J. Karel, A. Greer, G. Conti, S. Ueda, Y. Yamashita, M. Kobata, A. Yang, O. Sakata, and K. Kobayashi for hard x-ray photoemission measurements, and C. Antonakos, A. Ceballos, and A. Scholl for additional PEEM measurements at the ALS. This work was supported by the magnetism program at the Lawrence Berkeley National Laboratory, funded by the U.S. Department of Energy, Office of Basic Energy Sciences, Division of Materials Science and Engineering under Contract No. DE-AC02-05CH11231.

[1]M. Fallot and R. Hocart, Rev. Sci. **77**, 498 (1939).
[2]F. de Bergevin and L. Muldawer, Compt. Rend. **252**, 1347 (1961).
[3]J. S. Kouvel and C. C. Hartelius, J. Appl. Phys. **33**, 1343 (1962).
[4]L. M. Sandratskii and P. Mavropoulos, Phys. Rev. B **83**, 174408 (2011).
[5]M. Manekar and S. B. Roy, J. Phys. D: Appl. Phys. **41**, 192004 (2008).
[6]M. R. Ibarra and P. A. Algarabel, Phys. Rev. B **50**, 4196 (1994).
[7]S. Maat, J.-U. Thiele, and E. E. Fullerton, Phys. Rev. B **72**, 214432 (2005).
[8]J. Cao, N. T. Nam, S. Inoue, Y. Y. K. Hnin, N. N. Phuoc, and T. Suzuki, J. Appl. Phys. **103**, 07F501 (2008).
[9]M. Sharma, H. M. Aarbogh, J.-U. Thiele, S. Maat, E. E. Fullerton, and C. Leighton, J. Appl. Phys. **109**, 083913 (2011).
[10]N. T. Nam, W. Lu, and T. Suzuki, J. Appl. Phys. **105**, 07D708 (2009).
[11]J.-U. Thiele, S. Maat, and E. E. Fullerton, Appl. Phys. Lett. **82**, 2859 (2003).
[12]E. F. Kneller and R. Hawig, IEEE Trans. Magn. **27**, 3588 (1991).
[13]Y. Ding, D. A. Arena, J. Dovrak, M. Ali, C. J. Kinane, C. H. Marrows, B. J. Hickey, and L. H. Lewis, J. Appl. Phys. **103**, 07B515 (2008).
[14]R. Fan, C. J. Kinane, T. R. Charlton, R. Dorner, M. Ali, M. A. de Vries, R. M. D. Brydson, C. H. Marrows, B. J. Hickey, D. A. Arena, B. K. Tanner, G. Nisbet, and S. Langridge, Phys. Rev. B **82**, 184418 (2010).
[15]C. Baldasseroni, C. Bordel, A. X. Gray, A. M. Kaiser, F. Kronast, J. Herrero-Albillos, C. M. Schneider, C. S. Fadley, and F. Hellman, Appl. Phys. Lett. **100**, 262401 (2012).
[16]M. Loving, M. A. de Vries, F. Jimenez-Villacorta, C. Le Graët, X. Liu, R. Fan, S. Langridge, D. Heiman, C. H. Marrows, and L. H. Lewis, J. Appl. Phys. **112**, 043512 (2012).
[17]L. J. Swartzendruber, Bull. Alloy Phase Diagrams **5**, 456 (1984).
[18]M. Takahashi and R. Oshima, Mater. Trans., JIM **36**, 735 (1995).
[19]S. Hashi, S. Yanase, Y. Okazaki, and M. Inoue, IEEE Trans. Magn. **40**, 2784 (2004).
[20]K. M. Cher, T. J. Zhou, and J. S. Chen, IEEE Trans. Magn. **47**, 4033 (2011).
[21]S. Yuasa, Y. Otani, H. Miyajima, and A. Sakuma, J. Magn. Jpn. **9**(6), 202–209 (1994).
[22]P. H. L. Walter, J. Appl. Phys. **35**(3 Pt. 2), 938 (1964).
[23]J. S. Kouvel, J. Appl. Phys. **37**(3), 1257 (1966).
[24]W. Lu, N. T. Nam, and T. Susuki, IEEE Trans. Magn. **45**, 2716 (2009).
[25]S. A. Makhlouf, T. Nakamura, and M. Shiga, J. Magn. Magn. Mater. **135**(3), 257 (1994).
[26]R. Barua, F. Jimenez-Villacorta, and L. H. Lewis, Appl. Phys. Lett. **103**, 102407 (2013).
[27]W. Lu, B. Yan, and T. Suzuki, Scr. Mater. **61**, 851 (2009).
[28]W. Lu, N. T. Nam, and T. Susuki, J. Appl. Phys. **105**, 07A904 (2009).
[29]B. D. Cullity and S. R. Stock, *Elements of X-Ray diffraction*, 3rd ed. (Pearson Education, Prentice Hall, 2001).
[30]E. Yang, D. E. Laughlin, and Z. Jian-Gang, IEEE Trans. Magn. **48**(1), 7 (2012).
[31]C. F. Majkrzak, Physica (Amsterdam) **221B**, 342 (1996).
[32]P. A. Kienzle, J. Krycka, N. Patel, and I. Sahin, REFL1D (Version 0.6.19) [Computer Software], College Park, MD, 2011.
[33]S. R. Spurgeon, J. D. Sloppy, R. Tao, R. F. Klie, S. E. Lofland, J. K. Baldwin, A. Misra, and M. L. Taheri, J. Appl. Phys. **112**, 013905 (2012).
[34]C. Martinez-Boubeta, L. Balcells, and B. Martinez, J. Appl. Phys. **113**, 123908 (2013).
[35]S. Kim, F. Jona, and P. M. Marcus, Surf. Rev. Lett. **6**, 133 (1999).
[36]S. Lounis, M. Benakki, and C. Demangeat, Phys. Rev. B **67**, 094432 (2003).
[37]I. Suzuki, T. Koike, M. Itoh, T. Taniyama, and T. Sato, J. Appl. Phys. **105**, 07E501 (2009).
[38]G. C. Han, J. J. Qiu, Q. J. Yap, P. Luo, D. E. Laughlin, J. G. Zhu, T. Kanbe, and T. Shige, J. Appl. Phys. **113**, 17C107 (2013).
[39]G. C. Han, J. J. Qiu, Q. J. Yap, P. Luo, T. Kanbe, T. Shige, D. E. Laughlin, and J. G. Zhu, J. Appl. Phys. **113**, 123909 (2013).
[40]A. V. Ruban, H. L. Skriver, and J. K. Norskov, Phys. Rev. B **59**, 15990 (1999).
[41]K. Heinz and L. Hammer, J. Phys.: Condens. Matter **11**, 8377 (1999).
[42]J.-S. Lee, E. Vescovo, L. Plucinski, C. M. Schneider, and C.-C. Kao, Phys. Rev. B **82**, 224410 (2010).
[43]M. J. McLaren, M. A. de Vries, R. M. D. Brydson, and C. Marrows, J. Phys.: Conf. Ser. **371**, 012031 (2012).